Electrostatic interaction of a spherical particle in the vicinity of a circular orifice*

Lian Zeng-Ju(连增菊)†

Department of Physics, Ningbo University, Ningbo 315211, *China*

(Received 5 September 2009; revised manuscript received 7 December 2009)

The electrostatic interaction of a charged spherical particle in the vicinity of an orifice plane has been investigated in this paper. The particle can creep along the axis of the orifice and is immersed in a bulk electrolyte. By solving the Poisson–Boltzmann problem, we have obtained the effective electrostatic interaction for several values of reduced orifice radius $\tilde{h}$, including the cases of $\tilde{h} > 1$, $\tilde{h} = 1$ and $\tilde{h} < 1$. Two kinds of boundary conditions of the orifice plane are considered. One is the constant potential model corresponding to a conducting plane, the other is the constant charge model. In the constant potential model, there is an electrostatic attraction between the particle and the orifice plane when they get close to each other, while there is a pure electrostatic repulsion in the constant charge model. The interactions in both boundary models are sensitive to the parameters of the reduced orifice radius, the reduced particle–orifice distance, surface charge densities of the particle and orifice plane, and the reduced Debye screen constant corresponding to the salt-ion concentration and ion valence.

Keywords: colloid movement, electrostatic interaction, orifice radius, particle–orifice distance
PACC: 8270D, 7115Q

1. Introduction

The electrostatic interaction in colloidal solutions plays a crucial role in determining the structure and stability of the colloid dispersions or colloid aggregates.[1−3] When the colloidal suspension involved is very dilute, the interaction between particles can be neglected. Then, the interaction between charged particles and boundaries becomes one of the most important factors in determining the colloid movement.

Investigation of the electrostatic interaction between colloidal particles and various geometric boundaries has been made over the past several decades. The effect of the presence of a planar solid boundary was first examined by Morrison and Stukel[4] in their study on a hard particle, which was re-examined later by Keh *et al.*[5] and corrected some mistakes involved. The electrostatic interaction of a colloidal sphere in some other fixed boundaries, such as in a long circular tube and along the centre line between two large parallel plates, have also been theoretically studied under the assumption of infinitely thin double layer by Keh group.[6] In 1997, Ennis and Anderson[7] extended the scope of Keh group further to the finite double layer thickness, but the edge of the double layer was not allowed to touch the planar boundary. Fortunately, this problem was soon solved by Shugai and Carnie.[8] In their study, no restriction of double layer thickness was imposed and the double layer of the particle was allowed to touch the planar boundary. Additionally, different from Refs. [4] and [5], a 'soft' particle was investigated in the electrostatic interaction of this particle normal to a plane by Cheng *et al.*[9] This 'soft' particle consisted of an inner hard core coated with a concentric porous layer containing uniformly distributed fixed charges. In recent years, the effect of the boundary of a spherical cavity on the electrostatic interaction was also studied.[10,11]

Though various geometric boundary-corrected effects on the electrostatic interaction of colloidal solutions have been involved in the previous investigations, the study of the systems that possess much more complex boundaries, such as a colloidal suspension with porous boundary, is still open. The colloid movement in the suspension, such as electrophoresis and attachment, through an orifice or a porous medium has a great potential in industrial applications and also is of great significance in a number of environmental fields including contaminant transport, soil profile

*Project supported by the National Natural Science Foundation of China (Grant Nos. 10805029 and 10947175) , the Education Department of Natural Science Foundation of Zhejiang province of China (Grant No. Y200803420), and the Science Foundation of Ningbo University (Grant No. xkl09057), and sponsored by K.C.Wong Magna Fund in Ningbo University of China.
†Corresponding author. E-mail: lianzengju@nbu.edu.cn
© 2010 Chinese Physical Society and IOP Publishing Ltd

development, and subsurface migration of pathogenic microorganisms.[12−15] Meanwhile, the colloid movement through an orifice or a porous medium is also concerned with for mimicking a transmembrane transport of biomacromolecules which is an indispensable process to lives.[16]

The electrostatic interaction of colloidal particle restricted by an orifice in a large conducting plane has been investigated by Keh and Lien[17] for the first time. Unfortunately, this analysis was insufficient because of their employing of approximations. An assumption of thin double layers adjacent to solid surfaces was employed throughout their calculation. The size effect of charged particle was neglected and the boundary condition of the charged particle surface was simplified as a homogeneous boundary. In this paper, using the Poisson–Boltzmann theory and considering the size effect of particle and the exact boundary conditions of particle surface, we make a systematic examination of the axisymmetric electrostatic interaction of a charged particle creeping along the axis of an orifice in an infinite plane. Two kinds of boundary conditions of the orifice plane are considered in this paper. One is the constant potential model (corresponding to a conducting plane), and the other is the constant charge model. In the calculation, we find that there is an electrostatic attraction between the colloid and orifice in the constant potential model, while there is a pure repulsion in the constant charge model. Meanwhile, these electrostatic interactions are sensitive to the reduced colloid–orifice distance, Debye screen length, reduced orifice radius, and charge densities of the particle and orifice plane.

The paper is organized as follows. In Section 2, the model and theory of electrostatic interaction of a sphere along the axis of an orifice is described. The formulation of the potentials of the system and the solution scheme are given in Section 3. Based on the analysis in the previous sections, numerical solutions for the electrostatic energy of the system are obtained in Section 4. Section 5 gives the summary of the paper.

2. Model and theory

2.1. The electric potential of the system

Here, we consider a charged spherical particle with radius a in the vicinity of a plane with a circular orifice of radius h on it, as shown in Fig. 1. This particle can creep along the axis of the circular orifice. The system is immersed in an electrolyte with coions and counterions of valence z_0, modeled by a dielectric continuum of dielectric constant $\epsilon_{\rm e}$. For convenience of calculation, we divide the system into three parts: part I corresponds to the region of electric solution of $z < d$ including the colloidal particle, part II denotes the region of electric solution of $z > d$, and part III is the region inside the particle. We also denote the boundary with the Cartesian coordinate $z = d,\ \rho > h$ by G_w (not including the circular orifice), the surface of circular orifice ($z = d, \rho \leq h$) by G_0, and the surface of the particle by $G_{\rm p}$. Here, (ρ, z, ψ) and (r, θ, ψ) denote the circular cylindrical coordinates and the spherical coordinates respectively. The origins of these two coordinates are both chosen at the sphere centre. The electric potentials $\Psi_{\rm I}$ and $\Psi_{\rm II}$ in regions I and II are determined for a given particle-orifice distance d by solving the mean-field Poisson–Boltzmann (PB) equation, and $\Psi_{\rm III}$ in region III satisfies Laplace equation. For a 1 : 1 symmetric electrolyte system, the PB equation can be written as

$$\nabla^2 \Phi_i(\boldsymbol{r}) = z_0 b^2 \sinh\left(z_0 \Phi_i(\boldsymbol{r})\right), \quad i = \mathrm{I}, \mathrm{II} \tag{1}$$

and the Laplace equation reads

$$\nabla^2 \Phi_{\rm III}(\boldsymbol{r}) = 0, \tag{2}$$

where $\Phi_i = e\beta\Psi_i,\ i = \mathrm{I}, \mathrm{II}, \mathrm{III}$ (e being the elementary charge) are the normalised potentials, $b^2 = 2c_0\lambda_{\rm B}$ is related to a salt-ion concentration c_0, and $\lambda_{\rm B} = {\rm e}^2\beta/\epsilon_{\rm e}$, with $\beta = 1/k_{\rm B}T$, is the Bjerrum length and $k_{\rm B}$ is the Boltzmann constant.

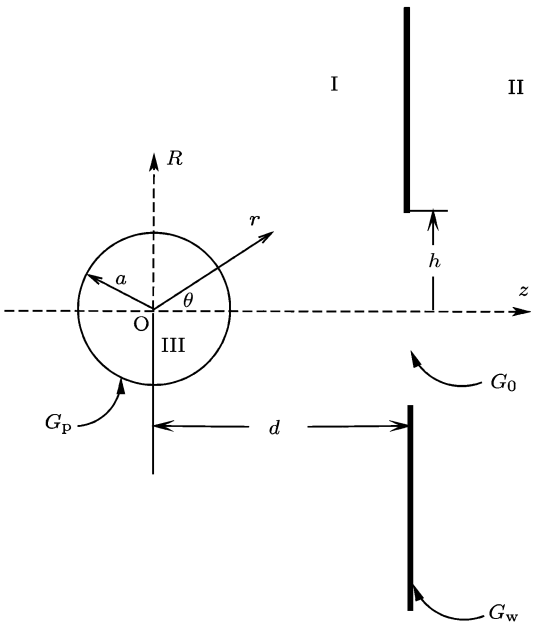


Fig. 1. A spherical particle creeping along the axis of a circular orifice.

The charges on the colloid surface or the surface of the plane enter the problem through the boundary conditions in the PB boundary value problem (BVP). We employ the constant-charge boundary condition which requires that the normal gradient of the electric potential is proportional to the particle surface charge density $\sigma_{\rm p}e$ at surface $G_{\rm p}$, i.e.

$$(\tau\nabla\Phi_{\rm III}(\boldsymbol{r})-\nabla\Phi_{\rm I}(\boldsymbol{r}))\cdot\boldsymbol{n}_{\rm p}=\lambda_{\rm B}\sigma_{\rm p},\quad \boldsymbol{r}\in G_{\rm p}, \tag{3}$$

$$\Phi_{\rm I}(\boldsymbol{r})=\Phi_{\rm III}(\boldsymbol{r}),\quad \boldsymbol{r}\in G_{\rm p}. \tag{4}$$

The second equation is the continuity condition of the surface potential. Here, $\boldsymbol{n}_{\rm p}$ is an outer normal unit vector of surface $G_{\rm p}$ and $\tau=\epsilon_{\rm p}/\epsilon_{\rm e}$ is a ratio between the dielectric constants of the particle and solution.

On the surface of the orifice plane, the boundary conditions are complicated, which are determined by the structure and property of the orifice plane. Here, we consider two extreme situations: (a) constant surface potential model for the surface of the orifice plane corresponding the conducting plane; (b) constant surface charge model for the surface of the orifice plane.

(a) Constant surface potential model for the surface of the orifice plane

Since the plane extends to infinity and is an equipotential surface, we set the electric potential at $G_{\rm w}$ and the infinity as the electric potential reference point. It is emphasized that the electric potential at the orifice (the surface of G_0) is not necessary to be zero, which can be defined in a general form as $\Phi_{\rm I}|_{G_{0<}}=\Phi_{\rm II}|_{G_{0>}}=f(\rho)$. Meanwhile, the current flux is continuous for $\rho<h$. The boundary conditions on the surface of the orifice plane then can be summarized as follows:

$$\Phi_{\rm I}(\boldsymbol{r})=\Phi_{\rm II}(\boldsymbol{r})=\begin{cases} f(\rho), & \boldsymbol{r}\in G_0,\\ 0 & \boldsymbol{r}\in G_{\rm w},\end{cases} \tag{5}$$

$$\nabla\Phi_{\rm I}(\boldsymbol{r})=\nabla\Phi_{\rm II}(\boldsymbol{r}),\qquad \boldsymbol{r}\in G_0. \tag{6}$$

(b) Constant surface charge model for the surface of the orifice plane

In this case, the normal gradient of the electric potential on the orifice plane is proportional to the surface charge density $\sigma_{\rm w}e$. The potential and current flux at the orifice are also continuous.

$$\Phi_{\rm I}(\boldsymbol{r})=\Phi_{\rm II}(\boldsymbol{r})=f_0(\rho),\qquad \boldsymbol{r}\in G_{\rm w},G_0, \tag{7}$$

$$(\nabla\Phi_{\rm I}(\boldsymbol{r})-\nabla\Phi_{\rm II}(\boldsymbol{r}))\cdot\boldsymbol{n}_{\rm w}=\begin{cases}\lambda_{\rm B}\sigma_{\rm w}, & \boldsymbol{r}\in G_{\rm w},\\ 0, & \boldsymbol{r}\in G_0,\end{cases} \tag{8}$$

where $\boldsymbol{n}_{\rm w}$ is an outer normal unit vector of surface $G_{\rm w}$.

Additionally, for both the constant surface potential model and constant surface charge model, the potentials in the regions I and II are finite as $z\to-\infty$ and $z\to\infty$ respectively. Meanwhile, since we set the potential in the infinity as the electric potential reference point for both models, we have

$$\Phi_{\rm I}(\boldsymbol{r})=0,\qquad z\to-\infty, \tag{9}$$

$$\Phi_{\rm II}(\boldsymbol{r})=0,\qquad z\to+\infty. \tag{10}$$

Finally, the whole system must be electroneutral. This condition is automatically satisfied when the above boundary conditions (3)–(10) are satisfied simultaneously for both models (a) and (b).

2.2. Electrostatic interaction energy of the system

The electrolyte in this paper is assumed to be unbounded, i.e. there is a reservoir of salt ions coupled to the system, so that the number of ions is not fixed. The fixed thermodynamics variables are: the temperature T, the chemical potential μ_0 for a given salt-ion concentration ($\beta\mu_0=\log c_0\Lambda^3$ with Λ the thermal wavelength), and the volume of the electrolyte region V. Our system is then in a grand canonical ensemble with the grand potential, Ω, being the relevant thermodynamic function. The grand potential then can be written in its final form[18,19]

$$\begin{aligned}\beta\Omega=&\frac{\sigma_{\rm p}}{2}\int_{G_{\rm p}}{\rm d}S\,\Phi_{\rm I}+\frac{\sigma_{\rm w}}{2}\int_{G_{\rm w}}{\rm d}S\,\Phi_{\rm I}\\&+\frac{b^2}{2\lambda_{\rm B}}\sum_{\rm I=I,II}\int_{\rm I}{\rm d}V(z_0\Phi_i\sinh z_0\Phi_i\\&-2\cosh z_0\Phi_i+2).\end{aligned} \tag{11}$$

Here, the first term gives the electrostatic energy due to the fixed colloidal charges on $G_{\rm p}$, the second term is due to the fixed orifice plane charges on $G_{\rm w}$ (this term vanishes for $\Phi_{\rm I}|_{z=d,\rho>h}=\Phi_{\rm II}|_{z=d,\rho>h}=0$ in the constant surface potential model), and the third term incorporates the entropic and electrostatic contributions of the mobile ions in regions I and II. The effective particle–orifice plane interaction energy W can now be defined as

$$W=\Omega-\Omega_\infty. \tag{12}$$

Ω_∞ is determined by solving the PB problem when the distance between the particle and orifice plane is infinite.

3. Formulation for the electric potentials of the system

Under the given boundary conditions (3)–(10), solving the PB equation (1) and Laplace equation (2), we can obtain the explicit potentials of the system. However, it is formidable to gain analytic solutions of Eq. (1) since it is nonlinear. (It usually can be solved numerically by finite element methods or some other numerical technique.) When the electric potential of the system is weak enough, the PB equation can be linearized

$$\nabla^2 \Phi_i(\boldsymbol{r}) - \kappa^2 \Phi_i(\boldsymbol{r}) = 0, \quad i = \mathrm{I}, \mathrm{II}, \tag{13}$$

where $\kappa^2 = (z_0 b)^2 = 2c_0 z_0^2 \lambda_{\mathrm{B}}$ is the screening parameter. Since the spherical particle is located on the axis of the circular orifice and is uniformly charged, the system is an axisymmetric one. That is to say, the electric potentials of the system (including that in regions I, II and III) are independent of the rotation angle ψ. Following an idea of the multipole expansion method,[20,21] the electric potential Φ_{I} in region I can be expanded in terms of basis functions.

$$\begin{aligned}\Phi_{\mathrm{I}} = &\sum_l A_l k_l(\kappa r) P_l(\cos\theta) \\ &+ \int_0^\infty F(\mu)\mu J_0(\mu\rho)\mathrm{e}^{\sqrt{\mu^2+\kappa^2}z}\mathrm{d}\mu, \\ &l = 0, 1, 2, \ldots, \infty,\end{aligned} \tag{14}$$

where $k_l(\kappa r)$ is defined as the modified spherical Bessel function of the second kind, $P_l(\cos\theta)$ denotes the Legendre polynomial of order l, $J_0(\mu\rho)$ is the Bessel function of the first kind of order zero, A_l are unknown constant coefficients and $F(\mu)$ is an unknown function of μ. Each part of Eq. (14) is a linear superposition of the complete solutions of Eq. (13). The first part of this equation written in spherical coordinates denotes the potential due to the charged particle, and the second part written in cylindrical coordinates represents the disturbances generated by the orifice plane.

In the region $z \geq d$, it is sufficient to represent all the disturbances generated at the plane $z = d$ by a Fourier–Bessel integral like the form given in Eq.(14).

$$\Phi_{\mathrm{II}} = \int_0^\infty G(\mu)\mu J_0(\mu\rho)\mathrm{e}^{-\sqrt{\mu^2+\kappa^2}z}\mathrm{d}\mu, \tag{15}$$

where $G(\mu)$ is an unknown function of μ. Note that a solution of the forms of Φ_{I} and Φ_{II} given by Eqs. (14) and (15) immediately satisfies the boundary conditions (9) and (10).

The electric potential in the particle which satisfies Eq. (2) can be expressed in terms of the basis functions with the spherical coordinates.

$$\Phi_{\mathrm{III}} = \sum_l B_l r^l P_l(\cos\theta), \quad l = 0, 1, 2, \ldots, \infty, \tag{16}$$

where B_l are unknown constant coefficients.

The unknown coefficients A_l and B_l and functions $F(\mu)$ and $G(\mu)$ in Eqs.(14)–(16) are determined by the boundary conditions (3)–(10). However, the accuracy is low when we solve the two unknown functions $F(\mu)$ and $G(\mu)$ directly by numerical calculation. Fortunately, this problem can be avoided by some analytical inversions. At first, the boundary condition (5) or (7) is satisfied along the orifice plane in each region for both models. After an inverse Hankel transform, the unknown functions $F(\mu)$ and $G(\mu)$ can be determined in terms of the coefficients A_l and the unknown potential profile $f(\rho)$ or $f_0(\rho)$ at the orifice. Then, by matching the current flux equation (6) or (8) at the orifice, the unknown orifice potential can be obtained in terms of the coefficients A_l. Finally, using the collocation technique described in Refs. [20] and [22], the numerical values of the coefficients A_l and B_l can be provided by satisfying the boundary conditions (3) and (4) on the surface of the sphere. We now give the specific solving process for these two cases of orifice plane boundaries respectively.

3.1. The solution of the potential for the constant potential model of the orifice plane

Substituting the electric potentials Φ_{I} and Φ_{II} into the plane boundary condition (5) for the constant potential model of the orifice plane and making an inverse Hankel transform, we obtain

$$F(\mu) = \mathrm{e}^{-\sqrt{\mu^2+\kappa^2}d}\left[f^*(\mu) - \sum_{l=0}^{\infty} A_l H_1^*(l,\mu)\right], \tag{17}$$

$$G(\mu) = \mathrm{e}^{\sqrt{\mu^2+\kappa^2}d} f^*(\mu), \tag{18}$$

where

$$f^*(\mu) = \int_0^h f(\rho)\rho J_0(\mu\rho)\mathrm{d}\rho, \tag{19}$$

$$H_1^*(l,\mu) = \int_0^\infty k_l(\kappa r) P_l(\cos\theta)\, \rho J_0(\mu\rho)\mathrm{d}\rho, \tag{20}$$

here, $f(\rho)$ is the unknown electric potential profile at the orifice which has been mentioned in Eq. (5). Applying the continuous condition of current flux on surface G_0 in Eq. (6), we obtain

$$f^*(\mu) = \frac{1}{2}\sum_{l=0}^{\infty} A_l H_1^*(l,\mu) - \frac{1}{2\sqrt{\mu^2+\kappa^2}}\sum_{l=0}^{\infty} A_l H_2^*(l,\mu) \tag{21}$$

with

$$H_2^*(l,\mu) = \int_0^h \mathrm{d}\rho\rho J_0(\mu\rho)\left(k_l'(\kappa r)\kappa P_l(\cos\theta)\cos\theta + k_l(\kappa r)P_l'(\cos\theta)\frac{\sin^2\theta}{r}\right), \tag{22}$$

where $r = \sqrt{d^2+\rho^2}$, $\cos\theta = d/\sqrt{d^2+\rho^2}$, $k_l'(\kappa r) = \mathrm{d}k_l(x)/\mathrm{d}x|_{x=\kappa r}$ and $P_l'(\cos\theta) = \mathrm{d}P_l(x)/\mathrm{d}x|_{x=\cos\theta}$. Substituting Eq. (21) into Eqs. (17) and (18) and making once Hankel and inverse Hankel transform respectively, we obtain analytic expansions of $F(\mu)$ and $G(\mu)$ with coefficients A_l

$$F(\mu) = \frac{1}{2}\mathrm{e}^{-\sqrt{\mu^2+\kappa^2}d}\left[-\sum_{l=0}^{\infty} A_l H_1^*(l,\mu) - \frac{1}{\sqrt{\mu^2+\kappa^2}}\sum_{l=0}^{\infty} A_l H_2^*(l,\mu)\right], \tag{23}$$

$$G(\mu) = \frac{1}{2}\mathrm{e}^{\sqrt{\mu^2+\kappa^2}d}\left[\sum_{l=0}^{\infty} A_l H_1^*(l,\mu) - \frac{1}{\sqrt{\mu^2+\kappa^2}}\sum_{l=0}^{\infty} A_l H_2^*(l,\mu)\right]. \tag{24}$$

Finally, the values of coefficients A_l and B_l in the expansion of electric potentials of regions I and III in Eqs. (14) and (16) are determined by the boundary conditions on the particle surface with Eqs. (3) and (4). Applying these conditions to the Eqs. (14) and (16), we obtain a series of linear equations about A_l and B_l

$$\sum_{l=0}^{\infty} B_l a^l P_l(\cos\theta) - \sum_{l=0}^{\infty} A_l k_l(\kappa a)P_l(\cos\theta) = \chi_0^*(\theta), \tag{25}$$

$$\tau\sum_{l=0}^{\infty} B_l a^{l-1} l P_l(\cos\theta) - \sum_{l=0}^{\infty} A_l k_l'(\kappa a)\kappa P_l(\cos\theta) = \chi_1^*(\theta), \tag{26}$$

where

$$\begin{aligned}\chi_0^*(\theta) &= \int_0^{\infty} \mathrm{d}\mu F(\mu)\mathrm{e}^{\sqrt{\mu^2+\kappa^2}a\cos\theta}\mu J_0(\mu a\sin\theta),\\ \chi_1^*(\theta) &= \int_0^{\infty} \mathrm{d}\mu F(\mu)\mathrm{e}^{\sqrt{\mu^2+\kappa^2}a\cos\theta}\mu\left[\mu J_0'(\mu a\sin\theta)\sin\theta + \cos\theta\sqrt{\mu^2+\kappa^2}J_0(\mu a\sin\theta)\right] + \sigma\lambda_{\mathrm{B}}.\end{aligned} \tag{27}$$

In the calculations, $\chi_0^*(\theta)$ and $\chi_1^*(\theta)$ are regarded as functions independent of current A_l and B_l and determined only by given θ. So, to obtain explicit solutions of A_l and B_l, we must use an iteration method. First, for an initial guess of the coefficients A_l and B_l, $F(\mu)$ is obtained from Eq. (23) through fast Hankel transformation, then inserting the results into Eqs. (25) and (26) to form a set of linear equations for the unknown A_l and B_l, the results are used as input for the next iteration. This iteration will never stop until the difference between the solutions of the last two iterations converges to a desired accuracy. Here, the accuracy is specified as the relative error of the coefficients between iterations less then 10^{-7}. This simple iteration scheme generally converges to the desired accuracy after 8 to 14 iterations for this axisymmetric system when the particle is close to the orifice.

3.2. The solution of the potential for the constant charge model of the orifice plane

Following the procedure as described in previous subsection, the potential of the constant charge model can be implemented in a straightforward way. Substituting the electrostatic potentials in the regions I and II expressed in Eqs. (14) and (15) into the boundary conditions of charged orifice wall, Eqs. (7) and (8), and making some Hankel and inverse Hankel transforms, we gain the analytic expressions of Φ_{I} and Φ_{II} as functions of A_l,

$$\Phi_{\mathrm{I}} = \int_0^{\infty} \mathrm{d}\mu\frac{1}{2}\mathrm{e}^{\sqrt{\mu^2+\kappa^2}(z-d)}\left[H_0(\mu) - \sum_{l=0}^{\infty} A_l H_1^*(l,\mu)\right]\mu J_0(\mu\rho) + \sum_{l=0}^{\infty} A_l k_l(\kappa r)P_l(\cos\theta), \tag{28}$$

$$\Phi_{\mathrm{II}} = \int_0^{\infty} \mathrm{d}\mu\frac{1}{2}\mathrm{e}^{\sqrt{\mu^2+\kappa^2}(d-z)}\left[H_0(\mu) + \sum_{l=0}^{\infty} A_l H_1^*(l,\mu)\right]\mu J_0(\mu\rho), \tag{29}$$

where

$$H_0(\mu) = \frac{1}{\sqrt{\mu^2+\kappa^2}}\left[\frac{\sigma_{\rm w}}{\mu}\left(\delta(\mu) - hJ_1(h\mu)\right) - \sum_{l=0}^{\infty} A_l H_3^*(l,\mu)\right] \tag{30}$$

with

$$H_3^*(l,\mu) = \int_0^{\infty} {\rm d}\rho\rho J_0(\mu\rho)\left(k_l'(\kappa r)\kappa P_l(\cos\theta)\cos\theta + k_l(\kappa r)P_l'(\cos\theta)\frac{\sin^2\theta}{r}\right). \tag{31}$$

Here, $\delta(\mu)$ denotes Dirac delta function and $H_1^*(l,\mu)$ has been given in Eqs. (20).

Similarly, the values of coefficients A_l and B_l in the expansion of electric potentials of regions I and III in Eqs. (14) and (16) are determined by the boundary conditions on the particle surface with Eqs. (3) and (4). Applying these conditions to Eqs. (14) and (16), we obtain a series of linear equations for A_l and B_l

$$\sum_{l=0}^{\infty} B_l a^l P_l(\cos\theta) - \sum_{l=0}^{\infty} A_l k_l(\kappa a) P_l(\cos\theta) = \chi_2^*(\theta), \tag{32}$$

$$\tau\sum_{l=0}^{\infty} B_l a^{l-1} l P_l(\cos\theta) - \sum_{l=0}^{\infty} A_l k_l'(\kappa a)\kappa P_l(\cos\theta) = \chi_3^*(\theta), \tag{33}$$

where

$$\begin{aligned}\chi_2^*(\theta) &= \int_0^{\infty} {\rm d}\mu\frac{1}{2}\left[H_0(\mu) - \sum_{l=0}^{\infty} A_l H_1^*(l,\mu)\right]\mu J_0(\mu a\sin\theta){\rm e}^{\sqrt{\mu^2+\kappa^2}(a\cos\theta-d)},\\ \chi_3^*(\theta) &= \sigma\lambda_{\rm B} + \int_0^{\infty} {\rm d}\mu\frac{1}{2}\mu\left[\mu J_0'(\mu a\sin\theta)\sin\theta + \cos\theta\sqrt{\mu^2+\kappa^2}J_0(\mu a\sin\theta)\right]\\ &\quad\times\left[H_0(\mu) - \sum_{l=0}^{\infty} A_l H_1^*(l,\mu)\right]{\rm e}^{\sqrt{\mu^2+\kappa^2}(a\cos\theta-d)}.\end{aligned} \tag{34}$$

The definite integrals in above equations must be performed numerically, and the iteration method is also needed.

In the complete expansions of Eqs. (25) and (26) or Eqs. (32) and (33), there are infinite numbers of coefficients to be determined since $l \to \infty$, which is a formidable task. Fortunately, due to the continuity and finiteness of the electric potentials of the system, the coefficients of A_l and B_l will be convergent with number l. That is to say, these expansions can be truncated at some value of $l_{\max} = N$ in numerical calculations. In this case, we leave $2(N+1)$ numbers of coefficients to be determined. Using the collocation technique,[20−22] these coefficients can be determined by substituting $2(N+1)$ numbers of discrete set of points on the generating arc of the particle into Eqs. (25) and (26) or Eqs. (32) and (33). It is noticeable that each point on the particle's generatrix denotes a circle on the particle's surface due to the axisymmetry of the system. Since the truncated equations are approximations of the complete equations, different choices of points on the boundaries may give different solutions of the expansion coefficients. It is also possible that some sets of points result in equations with the solution not uniquely determined. This kind of questions have been studied in the context of viscous flow problems, and some useful guide lines of convergence analysis were available.[21,22] In our calculation, we choose the points by the guidance resulting from viscous flow studies and check the convergence by successive increase of the order of truncating and by the comparison of the results from different sets of points used in calculations. The accuracy of the truncation technique is principally a function of the relative spacing d/a. For the cases of $d/a = 1.1$ (for $h/a = 0.8$) and $d/a = 2.0$ (for $h/a = 1.5$), the numbers of collocation points $N = 30$ and $N = 20$ are sufficiently large to achieve this convergence.

4. Results and discussion

Once the electric potentials are given, the grand potential and the interaction energy between the charged particle and orifice plane can be obtained easily from Eqs. (11) and (12). The parameters that have been employed are: the Debye screening constant κ that describes the salt-ion concentrations c_0 and ion valence z_0, Bjerrum length $\lambda_{\rm B}$ that describes

the equilibrium temperature of the system T and the dielectric constant of electrolyte $\epsilon_{\rm e}$, the particle radius a, the orifice radius h, the particle–orifice distance d, and the surface charge densities of the particle and orifice plane, $\sigma_{\rm p}$ and $\sigma_{\rm w}$. Generally, water with $\epsilon_{\rm e} = 80\epsilon_0$ (ϵ_0 denotes the dielectric constant of vacuum) is used as the solvent, and the system is usually set at room temperature, i.e. $T = 300$ K. Hence, $\lambda_{\rm B} = {\rm e}^2/k_{\rm B}T\epsilon_{\rm e} = 0.875\times10^{-2}$ μm. Scaling all lengths by a, the system then is characterised by five independent parameters: $\tilde{h} = h/a$, $\tilde{\kappa} = \kappa a$, $\tilde{d} = d/a$, $\tilde{\sigma}_{\rm p} = a\sigma_{\rm p}\lambda_{\rm B}$, and $\tilde{\sigma}_{\rm w} = a\sigma_{\rm w}\lambda_{\rm B}$.

Figure 2 shows the interaction energy between the particle and orifice plane as a function of the reduced particle–orifice distance $\tilde{d}$ for different reduced orifice radius $\tilde{h}$. Two kinds of the boundary conditions of the orifice plane are given in this figure: the constant potential model and the constant charge model (the latter is shown in the inset). The solutions for the electrostatic energy of the same particle normal to an infinite plane as $\tilde{h} = 0$ are compared with the results for the limiting case as $\tilde{h} = 0.2 \to 0$. It can be found that the results for $\tilde{h} \to 0$ from the calculation in this paper agree remarkably well with the exact results of all relative spacings between the sphere and the plane wall. This agreement demonstrates the accuracy of the numerical solution obtained using the collocation technique introduced in the previous section. Additionally, examination of the data shown in Fig. 2 reveals an interesting feature. For the constant potential model of the orifice plane, the interaction energy decreases with reducing particle–orifice distance for all finite orifice radius, while it increases with the decrease of the particle–orifice distance for the constant charge model. That is to say, there is electrostatic attraction between the particle and orifice plane for the constant potential model, while there is pure electrostatic repulsion for the constant charge model. ($F \propto -\partial W/\partial d$, here F is electrostatic interaction force.) Meanwhile, these interaction forces will be enhanced when the sphere approaches to the orifice for both models. The different properties of these interaction forces between the particle and orifice plane for these two kinds of boundary model imply two opposite directions of the electrophoretic mobility for the particle in the vicinity of the orifice plane. Moreover, these interactions (including the attraction and repulsion) with nonzero orifice radius are all weaker than that for the system of an identical sphere close to an infinite plane. The interaction decreases with the increase of the reduced orifice radius $\tilde{h}$ for all relative spacings of the particle and orifice plane. This phenomenon is due to the decreasing effective wall-interaction areas that offer attraction or repulsion to the particle as the reduced orifice radius increases.

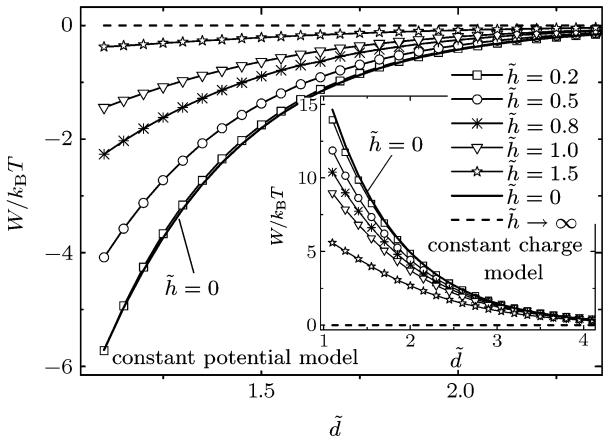


Fig. 2. The interaction energy of the charged particle and orifice plane as a function of reduced particle–orifice distance $\tilde{d}$ for different reduced orifice radius $\tilde{h}$. Two kinds of boundary conditions of the orifice plane are considered: the constant potential model and the constant charge model (shown in the inset). The reduced Debye screen parameter is $\tilde{\kappa} = 1.673$.

The electrostatic interaction energy of the charged particle and orifice plane versus the reduced particle–orifice distance for different reduced Debye screen constants corresponding to the reduced salt-ion concentrations $\tilde{c}_0$ and ion valence z_0 are plotted in Fig. 3 for both constant potential model and constant charge model. It can be found that the absolute values of the interaction energy for these two models are both enlarged with the decrease of the dimensionless salt-ion concentrations $\tilde{c}_0$. Meanwhile, monovalent ions can more remarkably enhance the electrostatic interaction of the charged particle and orifice plane than the divalent ions. That implies colloid electrophoresis will be more significant in the case of monovalent ions solution, such as Na^+, than that in the case of divalent ions solution, such as Ca^{2+}, which have been demonstrated by many papers.[23,24] It is noteworthy that the salt-ion $\tilde{c}_0$ and ion valence z_0 are not independent parameters. Different couples of $\tilde{c}_0$ and z_0 can result in the same electrostatic energy. In fact, reduced Debye screen constants $\tilde{\kappa} \propto |z_0|\tilde{c}_0^{1/2}$ determines exclusively the electrostatic energy when the other parameters such as $\tilde{h}$, $\tilde{d}$, $\tilde{\sigma}_{\rm p}$, and $\tilde{\sigma}_{\rm w}$ are fixed. In the inset of Fig. 3, comparisons of the electrostatic interaction energies with several couples of $\tilde{c}_0$ and z_0 are given for both the constant potential model and the constant

charge model. Obviously, the curves of the electrostatic energy agree remarkably with each other in the cases of identical $\tilde{\kappa}$ though they have different values of $\tilde{c}_0$ and z_0 such as the curves with $\tilde{c}_0 = 200, z_0 = 1$ and $\tilde{c}_0 = 50, z_0 = 2$, and have the same Debye screen constant $\tilde{\kappa} = 2.646$, as see in Fig. 3.

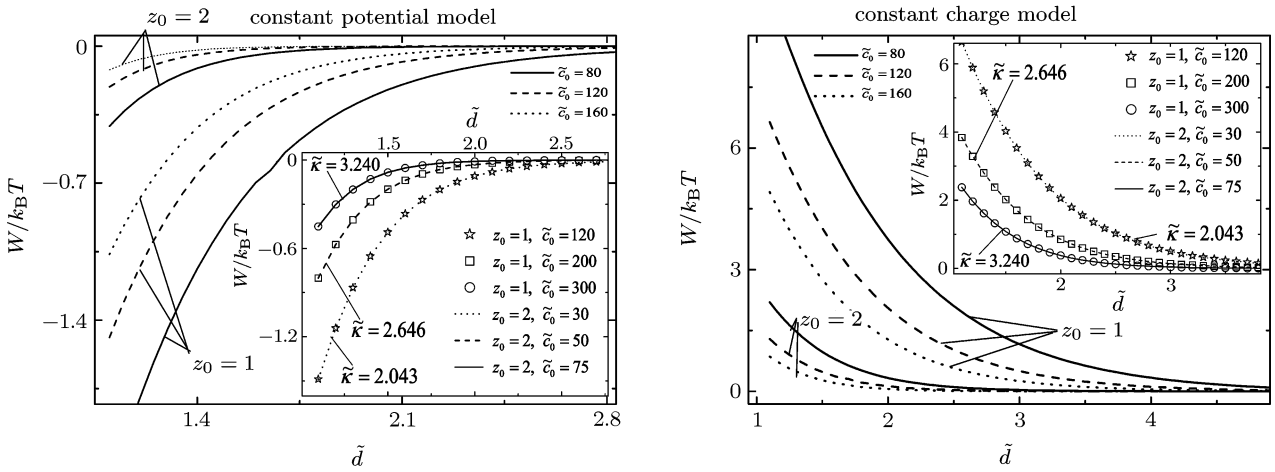


Fig. 3. The interaction energy of the charged particle and orifice plane versus the reduced particle–orifice distance for different reduced Debye screen constants corresponding to the reduced salt-ion concentrations $\tilde{c}_0$ and ion valence z_0. The reduced orifice radius is $\tilde{h} = 0.8$.

Except $\tilde{h}$, $\tilde{\kappa}$, and $\tilde{d}$, the reduced surface charge density of the particle $\tilde{\sigma}_{\rm p}$ is also an important factor in affecting the interaction energy. In Figs. 2 and 3, we set $\tilde{\sigma}_{\rm p} = 0.696$ corresponding to the total charges $Q = 500$, which is much lower than that in general experiments.[25–27] The selection of such a low surface charge density of the sphere is to ensure that the electric potential of the system are weak enough to be valid in the linear approximation. Figure 4 gives the interaction energy for difference surface charge densities of the particle for both the constant potential model and the constant charge model. It is obvious that the magnitudes of interaction are enhanced rapidly with the increase of reduced surface charge density of the particle. In the case of the constant charge model, the surface charge density of the orifice plane $\tilde{\sigma}_{\rm w}$ also has remarkable effect on the interaction energy. The energy is also enhanced with the increase of the charge density of the orifice plane, as shown in Fig. 5.

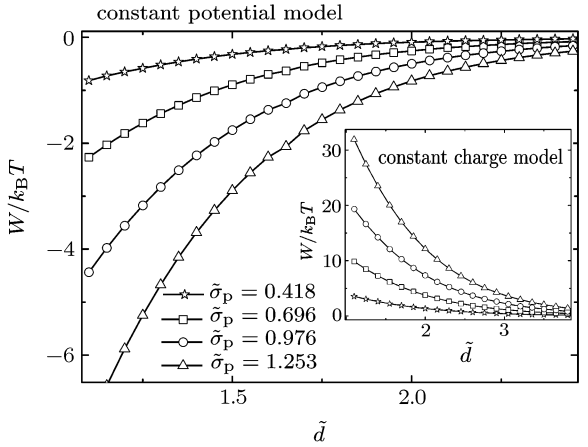


Fig. 4. The interaction energy of the charged particle and orifice plane as a function of reduced particle–orifice distance for different surface charge densities of the particle $\tilde{\sigma}_{\rm p}$. The other parameters are: $\tilde{h} = 0.8$, $\tilde{\kappa} = 1.673$.

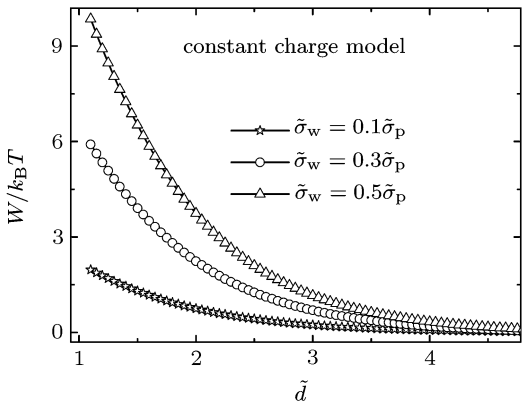


Fig. 5. The interaction energy of the charged particle and orifice plane versus reduced particle–orifice distance for different surface charge densities of the orifice plane $\tilde{\sigma}_{\rm w}$ for the constant charge model. The other parameters are: $\tilde{h} = 0.8$, $\tilde{\kappa} = 1.673$.

5. Summary

The electrostatic interaction of a colloidal sphere approaching a solid orifice plane or a porous film is often encountered in the colloid electrophoresis or any other colloid transportation in dielectric materials. It is important to understand if the solid surface significantly affects the electrostatic interaction of the spheres. In the present work, we have investigated the electrostatic interaction of a system with a charged spherical particle of radius a creeping along the axis of a circular orifice in an infinite plane. The system is immersed in a bulk electrolyte. Using the collocation technique described in Refs. [21] and [22], we have calculated the effective electrostatic interaction for various values of reduced orifice radius $\tilde{h}$, including the cases of $\tilde{h} > 1$, $\tilde{h} = 1$ and $\tilde{h} < 1$, by solving the PB BVPs. In the calculation, two kinds of boundary conditions of the orifice plane are considered. One is the constant potential model and the other is constant charge model. The results of the calculation show that there is electrostatic attraction between the charged particle and the orifice plane when they are close to each other in the constant potential model, while there is pure electrostatic repulsion in the constant charge model. Simultaneously, the effective electrostatic interaction is sensitive to the reduced orifice radius $\tilde{h}$ for both boundary models. Due to the decrease of effective wall-interaction areas that offer attraction or repulsion to the particle as it approaches the orifice, the interaction decreases with the increase of $\tilde{h}$. Additionally, the reduced Debye screen constant $\tilde{\kappa}$ (corresponding to ion-salt concentration $\tilde{c}_0$ and ion valence z_0) is also an important parameter in determining the electrostatic interaction between the charged particle and orifice plane. The interaction is enhanced more significantly when the system is immersed in a monovalent salt-ion solution than that in a divalent salt-ion solution when the ion-salt concentration is fixed. The solution with lower concentration of ion-salt is helpful to the electrostatic interaction between the charged particle and orifice plane. But whatever the z_0 and $\tilde{c}_0$ are, the electrostatic interaction will be fixed as long as $\tilde{\kappa} \propto |z_0|\tilde{c}_0^{1/2}$ is fixed.

In practical applications of electrophoresis or other colloid movement, the particles can approach an orifice in an off-centre path. It would be of interest to know whether the electrostatic forces tend to push the particle more off-centre or to bring it back to the centreline. This asymmetric problem is now under investigation and will be presented in a subsequent article.

References

[1] Gao H X, Huang L X and Xiao Ch M 2009 *Acta Phys. Sin.* **58** 5864 (in Chinese)
[2] Chen Sh L, Dong P and Liu R X 2009 *Acta Phys. Sin.* **58** 2820 (in Chinese)
[3] Huang L X, Xiao C M, Hu P and Gao H X 2009 *Chin. Phys.* B **18** 1287
[4] Morrison F A and Stukel J J 1970 *J. Colloid Interfac Sci.* **33** 88
[5] Keh H J, Lien L C and Chin J 1989 *Inst. Chem. Engin.* **20** 283
[6] Keh H J and Anderson J L 1985 *J. Fluid Mech.* **194** 417
[7] Ennis J and Anderson J L 1997 *J. Colloid Interface Sci.* **185** 496
[8] Shugai A A and Carnie S L 1999 *J. Colloid Interface Sci.* **213** 298
[9] Cheng W L, He Y Y and Lee E 2009 *J. Colloid Interface Sci.* **335** 130
[10] Yu H Y, Huang S H and Hsu J P 2004 *Colloid and Polymer Sci.* **283** 1
[11] Hsu J P, Chen Z S, Ku M H and Yeh L H 2007 *J. Colloid Interface Sci.* **314** 256
[12] Torkzaban S, Bradford S A, Genuchten M Th V and Walker S L 2008 *J. Conta. Hydrology* **96** 113
[13] McGechan M B and Lewis D R 2002 *Biosyst. Eng.* **83** 255
[14] Bradrford S A, Simunek J, Bettahar M, Genuchten M Th V and Yates A S 2003 *Environ. Sci. Technol.* **37** 2242
[15] Bringuier E and Bourdon A 2003 *Phys. Rev.* E **67** 011404
[16] Ito Y and Park Y S 2000 *Polym. Adv. Technol.* **11** 677
[17] Keh H J and Lien L C 1991 *J. Fluid Mech.* **224** 305
[18] Lian Z J and Ma H R 2007 *J. Chem. Phys.* **127** 104507
[19] Mbamala E C and von Grünberg H H 2002 *J. Phys.: Condens. Matter* **14** 4881
[20] Gluckman M J, Pfeffer R and Weinbaum S 1971 *J. Fluid Mech.* **50** 705
[21] Weinbaum S, Ganatos P and Yan Z Y 1990 *Ann. Rev. Fluid Mech.* **22** 275
[22] Lian Z J and Ma H R 2008 *J. Phys.: Condens. Matter* **20** 035109
[23] Felipe C, Morales L, Stranthmann M and Flemming H C 2007 *Water Research* **41** 2059
[24] Thomas F, Michot L J, Vantelon D, Montargès E, Prélot B, Cruchaudet M and Delon J F 1999 *Colloid Surfaces* A: *Physicochem. Eng. Aspects* **159** 351
[25] Crocker J C and Grier D G 1994 *Phys. Rev. Lett.* **73** 352
[26] Crocker J C and Grier D G 1996 *Phys. Rev. Lett.* **77** 1897
[27] Chen W, Tan S, Ng T K, Ford W T and Tong P 2005 *Phys. Rev. Lett.* **95** 218301